

## Threshold Effects in Proton-induced Reactions on Copper

Z. E. Switkowski,<sup>A</sup> J. C. P. Heggie<sup>A,B</sup> and F. M. Mann<sup>C</sup>

<sup>A</sup> School of Physics, University of Melbourne, Parkville, Vic. 3052.

<sup>B</sup> Present address: Department of Physical Sciences, St. Vincent's Hospital, Fitzroy, Vic. 3065.

<sup>C</sup> Hanford Engineering and Development Laboratory, Richland, Washington 99352, U.S.A.

### *Abstract*

A study has been made of proton-induced reactions on the two copper isotopes  $^{65}\text{Cu}$  and  $^{63}\text{Cu}$  for bombarding energies in the range 1.2–4.6 MeV. This energy range includes the (p,n) thresholds for  $^{65}\text{Cu}$  and  $^{63}\text{Cu}$ , which occur at 2.17 MeV and 4.21 MeV respectively. Excitation functions for (p, $\gamma$ ) reactions were obtained by observing discrete  $\gamma$ -ray transitions between low-lying states of the compound nuclei. Data were also obtained for the charged-particle reactions  $^{65}\text{Cu}(p,\alpha_0)^{62}\text{Ni}$  and  $^{63}\text{Cu}(p,\alpha_{0,1})^{60}\text{Ni}$ . As the respective (p,n) thresholds are crossed, the yields of proton-induced reactions on  $^{65}\text{Cu}$  fall by a factor of about 5 while the excitation functions of proton-induced reactions on  $^{63}\text{Cu}$  reveal no evidence of a significant threshold effect. These data are compared with Hauser–Feshbach statistical model calculations. The structure in the  $^{65}\text{Cu}+p$  reaction yield is interpreted in terms of Wigner cusps.

### 1. Introduction

There is considerable interest at present in the use of the Hauser–Feshbach statistical model for the prediction of nuclear reaction cross sections. Such calculations are pertinent to a wide variety of scientific and technological problems. As examples, we note the need to compute cross sections for reactions which have not been or cannot be measured in the laboratory but which are needed for calculations of nucleosynthesis in exploding stars (Fowler 1976). Also, calculated light-ion induced reaction rates are used extensively to estimate the buildup of radioactivity and to assess radiation damage effects in fission reactors (Mann and Schenter 1977). Similar calculations are required for design studies of controlled thermonuclear reactors (Mann and Switkowski 1975). Consequently, it is important that this model of nuclear reactions be verified by comparison with a wide range of experimental data.

The behaviour of nuclear reaction cross sections near thresholds is an especially sensitive test of the ability of the Hauser–Feshbach statistical model to predict the energy dependence of reaction cross sections. Wigner (1948) predicted that there should be a drop in cross section (Wigner cusp) for already open channels when a new channel opens. Thus, if the total reaction cross section varies smoothly with energy, the threshold effect should be most dramatic when a new channel opens, quickly absorbing an appreciable amount of the total flux, and when there are few already open channels which may share the resultant decrease in flux. Therefore, cusps might be most readily observed in the vicinity of s-wave neutron thresholds.

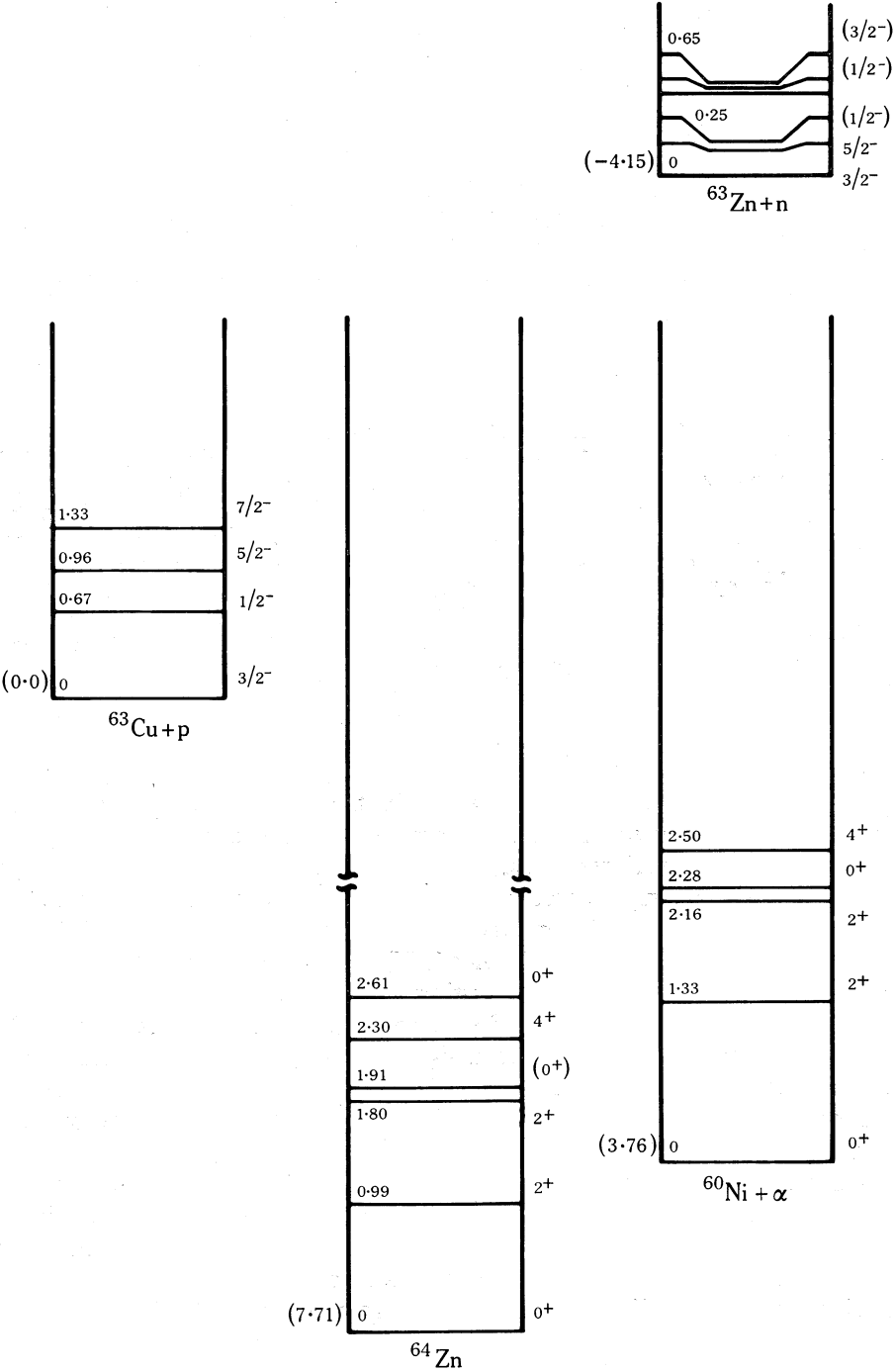


**Fig. 1.** Energy level schemes for the (a)  $^{63}\text{Cu} + p$  (above) and (b)  $^{65}\text{Cu} + p$  systems (opposite). The reaction  $Q$  values relative to the respective entrance channels are shown in parentheses.

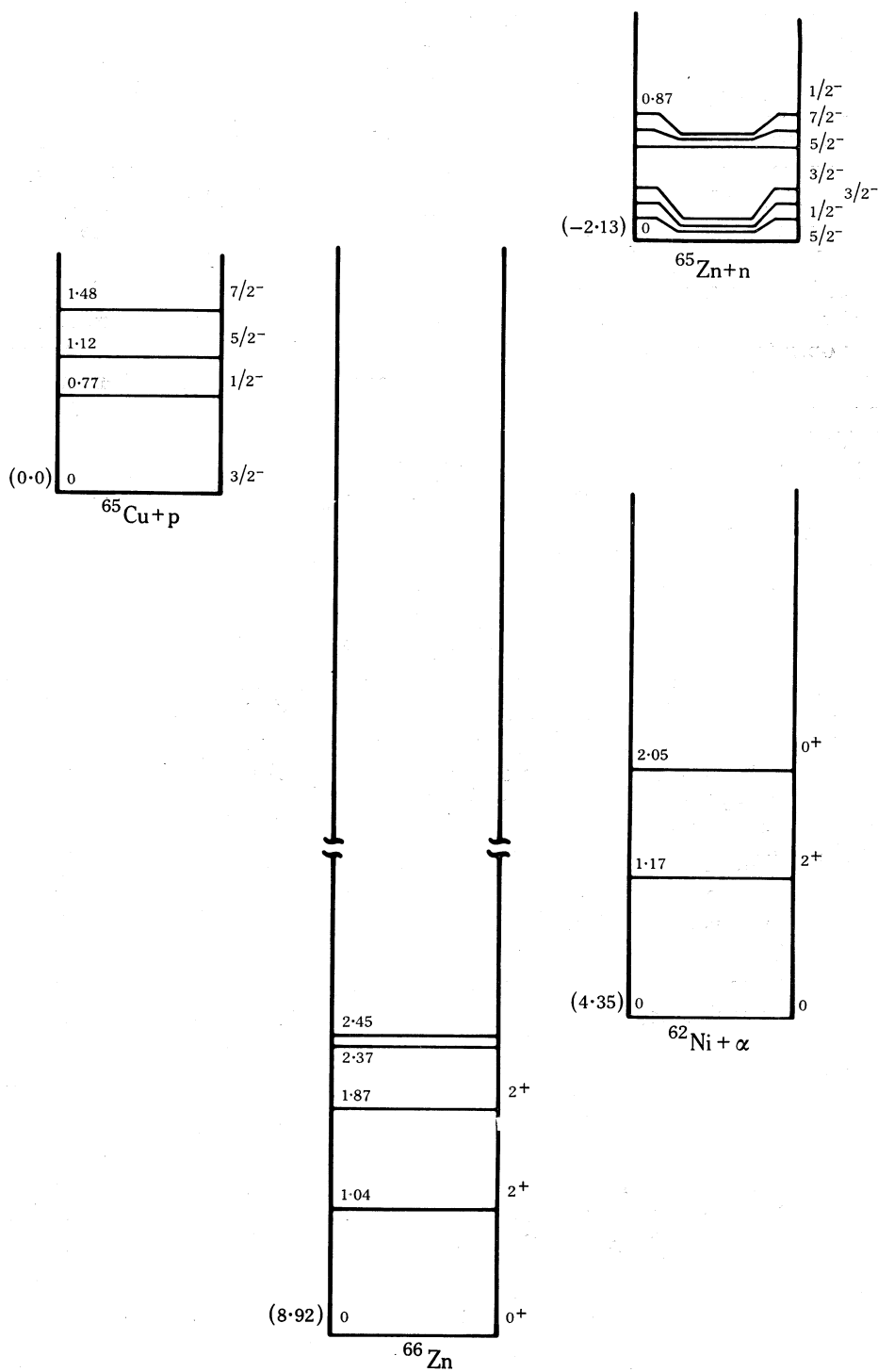


Fig. 1b

There are few examples in the literature of prominent threshold effects in charged-particle-induced reactions. Until recently, the only notable cases involved proton-induced reactions on the light elements  $^3\text{H}$  (Jarmie and Allen 1959),  $^7\text{Li}$  (Presser and Bass 1972) and  $^9\text{Be}$  (Votava and Thompson 1972). These elements are characterized by low-energy (p, n) thresholds. Renewed interest in these threshold phenomena was generated by Woosley *et al.* (1975) who, in a theoretical survey of 179 reactions of potential astrophysical importance, identified many examples of reactions expected to exhibit dramatic cusp-like features. Guided by these calculations, Mann *et al.* (1975) studied the  $^{64}\text{Ni}(p, \gamma)^{65}\text{Cu}$  reaction over an energy range which included the (p, n) threshold, and observed a spectacular cusp wherein the (p,  $\gamma$ ) cross section fell by an order of magnitude once the n channels were energetically open (see commentary by Hodgson 1976). Statistical model calculations using global parameter sets successfully reproduced these observations. Since then, attempts have been under way in several laboratories to identify further examples (see e.g. Zyskind *et al.* 1977).

In the present paper, we report a study of proton-induced reactions on the two copper isotopes  $^{63}\text{Cu}$  and  $^{65}\text{Cu}$ . The  $^{65}\text{Cu} + p$  system was identified by Woosley *et al.* (1975) as being of special interest because deep cusps were predicted in both the (p,  $\gamma$ ) and (p,  $\alpha$ ) reactions—a relatively uncommon occurrence. In contrast,  $^{63}\text{Cu} + p$  reaction cross sections were not expected to show any unusual energy dependence. These differing features may be understood in the context of the relevant energy level schemes displayed in Fig. 1. For the case of  $^{65}\text{Cu} + p$ , the n threshold is crossed at a proton energy of 2.17 MeV which is well down the Coulomb barrier. (Optical model calculations indicate that the transmission coefficient for s-wave proton capture by  $^{65}\text{Cu}$  is 0.5 at an energy of  $\sim 4.5$  MeV.) Consequently, the contribution of inelastic and compound-elastic scattering to the total reaction cross section is small. At these low energies the total reaction cross section is then composed only of (p,  $\gamma$ ) and (p,  $\alpha_0$ ) contributions. In addition, there is a high density of low-lying states in  $^{65}\text{Zn}$ , some of which may be populated by s-wave neutrons. Therefore, the successive opening of these channels over a small interval in the bombarding energy should result in a depletion of the (p,  $\gamma$ ) and (p,  $\alpha_0$ ) cross sections.

Using the symbolism of the statistical model, the above feature may be illustrated in the following manner. At a particular bombarding energy the fraction of the total cross section which populates the  $\gamma$ -ray channels is  $f$ , where

$$f \approx T_\gamma / \sum_\alpha T_\alpha. \quad (1)$$

Here,  $T_\gamma$  is an effective  $\gamma$ -ray transmission coefficient (defined in detail by Holmes *et al.* 1976) and the summation in the denominator extends over all open channels. Once the n threshold is crossed, the approximation (1) takes the form

$$f' \approx T_\gamma / \left( T_n + \sum_\alpha T_\alpha \right), \quad (2)$$

where the neutron transmission coefficient  $T_n$  has been explicitly indicated, and the

channels  $\alpha$  do not include the neutron channels. Now  $T_n \approx 1$  for s-wave neutrons of energy around a few hundred keV. Therefore, if

$$\sum_{\alpha} T_{\alpha} \ll 1$$

then

$$f' \ll f.$$

This is the case for  $^{65}\text{Cu} + p$ .

The different behaviour predicted for  $^{63}\text{Cu} + p$  may be attributed largely to the higher energy n threshold of 4.21 MeV. Although the (p,n) reaction may proceed via s-wave neutron emission, at this bombarding energy there are already a number of effectively open channels, namely, compound-elastic and inelastic scattering to low-lying  $^{63}\text{Cu}$  states, so that we have

$$\sum_{\alpha} T_{\alpha} \gtrsim T_n.$$

Under these circumstances,  $f'$  is not expected to be greatly different from  $f$ .

In Section 2 of the present paper experimental details are provided and the results are presented in Section 3. A discussion of the statistical model is given in Section 4 together with a comparison of the predictions with the experimental data. A brief description of the  $^{65}\text{Cu}(p, \gamma)$  and  $^{65}\text{Cu}(p, \alpha_0)$  reaction data has been published elsewhere (Switkowski *et al.* 1978).

## 2. Experimental Details

### (p, $\gamma$ ) Measurements

Targets were prepared by vacuum evaporation of 99.9% reagent grade copper. For the  $\gamma$ -ray yield measurements, the target consisted of  $500 \mu\text{g cm}^{-2}$  copper deposited on a 0.025 cm thick gold backing. Target thickness was determined from the mass change of the gold blank and also from the quartz crystal deposition monitor reading at the end of the evaporation. This target was mounted directly at the end of a stainless steel target chamber on a knife-edge seal at  $55^\circ$  to the beam direction. The  $\gamma$ -ray yields were measured with a  $60 \text{ cm}^3$  Ge(Li) detector positioned at  $55^\circ$  relative to the beam direction and with its front face parallel to the plane of the target and 1 cm away. A 3 mm lead absorber attenuated the low-energy  $\gamma$ -rays arising from the Coulomb excitation of the gold backing.

The (p,  $\gamma$ ) excitation functions were measured over the energy range from  $E_p = 1.2$  to 3.3 MeV in 100 keV steps from 1.2 to 1.8 MeV and in 50 keV steps thereafter. The target was 70 keV thick to a 2 MeV proton beam. This thickness was chosen in order to average over possible narrow resonances in the reaction cross section. Proton beams were delivered by the University of Melbourne 5U Pelletron accelerator and were defined by a 4 mm diameter aperture before striking the target. Beam intensity was reduced from 500 nA at the lower energies to 200 nA at the higher energies in order to maintain a reasonable counting rate for which the analyser dead time was  $<10\%$ . Data were acquired typically for 150  $\mu\text{C}$  of integrated charge. At each bombarding energy, spectra were recorded with a 4096 channel ADC and PDP-11/40 computer, and were stored on magnetic tape for off-line analysis.

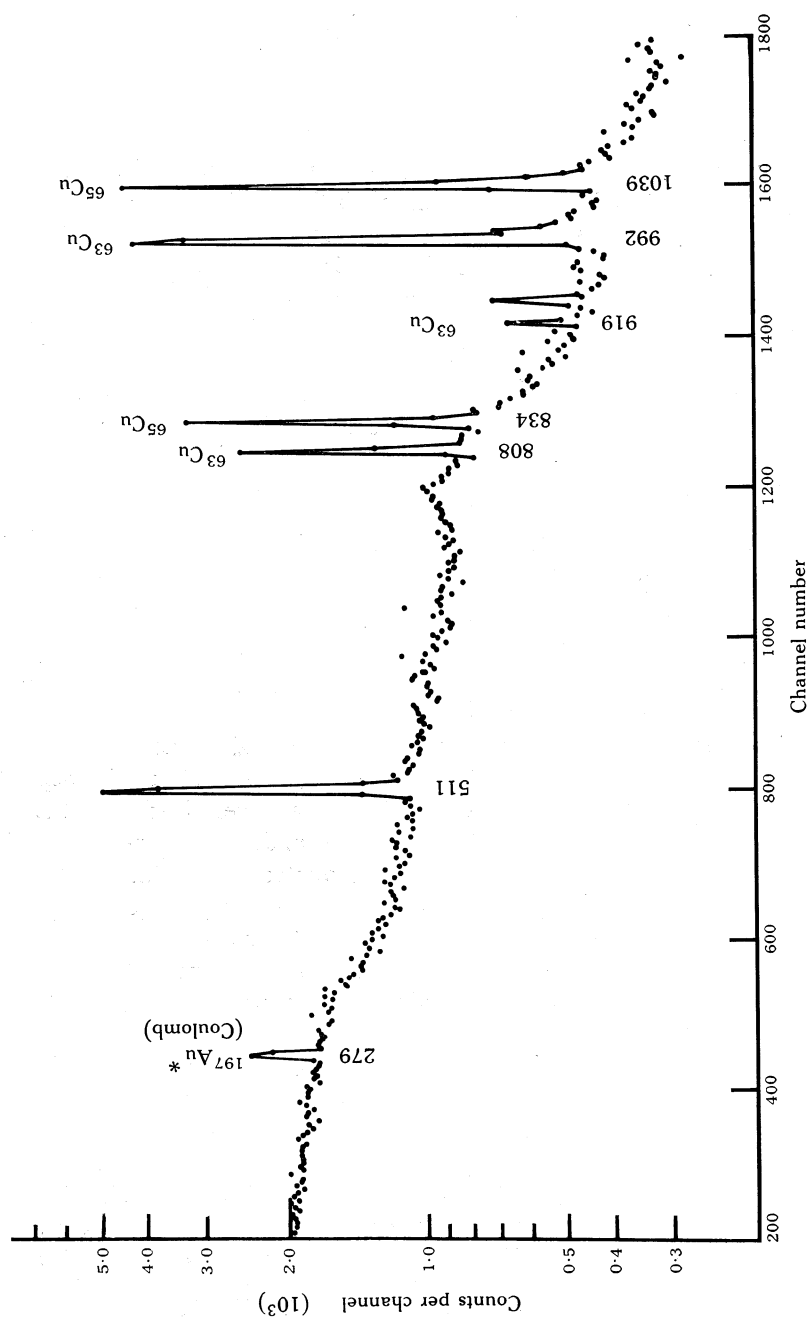


**Fig. 2.** Example of a  $\gamma$ -ray spectrum obtained with a 2 MeV proton beam incident on a thin natural copper target. Only every fifth channel is plotted. In addition to the 511 keV annihilation peak and the Au Coulomb excitation line, the spectrum is dominated by the indicated  $\gamma$ -ray photopeaks (energy in keV), with the identity of the Cu isotope involved noted alongside. The spectrum was acquired for a total integrated charge of 150  $\mu\text{C}$ .

### *(p, $\alpha$ ) Measurements*

Thin copper films were prepared by vacuum evaporation of copper onto glass slides coated with a release agent. These films were floated off and picked up onto Ta frames. The self-supporting target that was selected for the runs had a thickness of  $320 \mu\text{g cm}^{-2}$ . Alpha particles from  $(p, \alpha)$  reactions and scattered protons were detected with a  $300 \mu\text{m}$  silicon surface barrier-detector positioned at  $120^\circ$  and subtending a solid angle of  $5.8 \text{ msr}$ . The target thickness was determined from elastic scattering measurements carried out at proton energies between 1.5 and 2.3 MeV. The measured energy dependence of the yield of scattered protons was consistent with Rutherford scattering.

Data were acquired over the energy range 1.5 to 4.6 MeV in intervals of 100 keV except near the  $(p, n)$  thresholds where smaller steps of 50 keV were taken. The proton beam was collimated to a 2 mm diameter spot, and after passing through the target was collected in a Faraday cup. The current was typically 300 nA. Data were taken for a fixed integrated charge per point of typically  $300 \mu\text{C}$ . The absolute  $(p, \alpha)$  cross section was determined by normalization to the Rutherford scattering cross section after correcting for the normal isotopic abundances of the two isotopes. A description of the scattering chamber has been given elsewhere (Paine *et al.* 1978).

### *(p, n) Measurements*

Measurements of the relative neutron yield were made over the proton energy range 2.15 to 4.0 MeV, where contributions arose from only  $^{65}\text{Cu}(p, n)^{65}\text{Zn}$  reactions. The neutron detector consisted of a conventional  $^{10}\text{BF}_3$  counter imbedded in a paraffin moderator. The counter was mounted at  $0^\circ$  and close to the target which was the same as described above for the  $(p, \gamma)$  measurements. It was expected that, for energies sufficiently above the  $n$  threshold, the  $(p, n)$  reaction would have an isotropic yield, so that the observed yield would be a reasonably accurate measure of the total  $(p, n)$  cross section. Finally, the measured relative excitation function was normalized to the absolute data of Collé *et al.* (1974) whose experiment involved the measurement of the yield of delayed  $^{65}\text{Zn}$  activity.

## 3. Results

Fig. 2 displays a  $\gamma$ -ray spectrum measured at  $E_p = 2 \text{ MeV}$ . The portion of the spectrum at higher energies which is not shown was found to be relatively featureless. In addition to the 511 keV annihilation peak and the low energy Au Coulomb excitation line, the spectrum is dominated by only a few peaks corresponding to transitions between the low-lying states of the  $^{64}\text{Zn}$  and  $^{66}\text{Zn}$  compound nuclei. Reference to Fig. 1 shows that these lines arise between transitions involving only the ground state and first two excited states of each nucleus. The  $\gamma$ -ray photopeaks are clearly resolved and no confusion arises from the presence of two Cu isotopes in the target.

The ratio of the photopeak yields of the 1039 and 834 keV  $\gamma$ -rays in the case of  $^{66}\text{Zn}$  and 992 and 808 keV  $\gamma$ -rays in the case of  $^{64}\text{Zn}$  was constant to within  $\pm 5\%$  over the bombarding energy range investigated during this experiment. The relative  $(p, \gamma)$  cross sections were then defined as the measured excitation functions for the 1039 and 992 keV  $\gamma$ -rays for  $^{65}\text{Cu}$  and  $^{63}\text{Cu}$  respectively. Measurement of the  $^{63}\text{Cu}(p, \gamma)$  yield curve did not proceed beyond 3.2 MeV, due to the high  $\gamma$ -ray background yield of  $^{65}\text{Cu}(p, n\gamma)$  reactions and the excessive exposure of the Ge(Li)

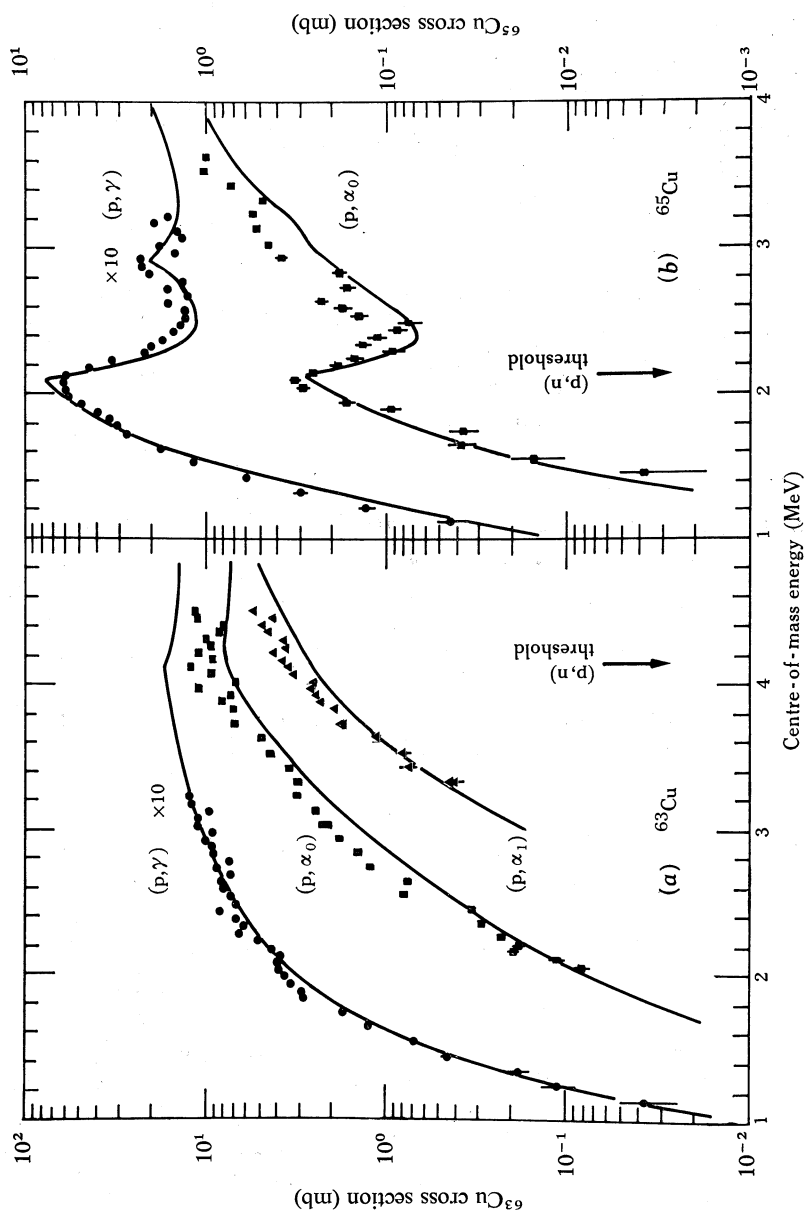
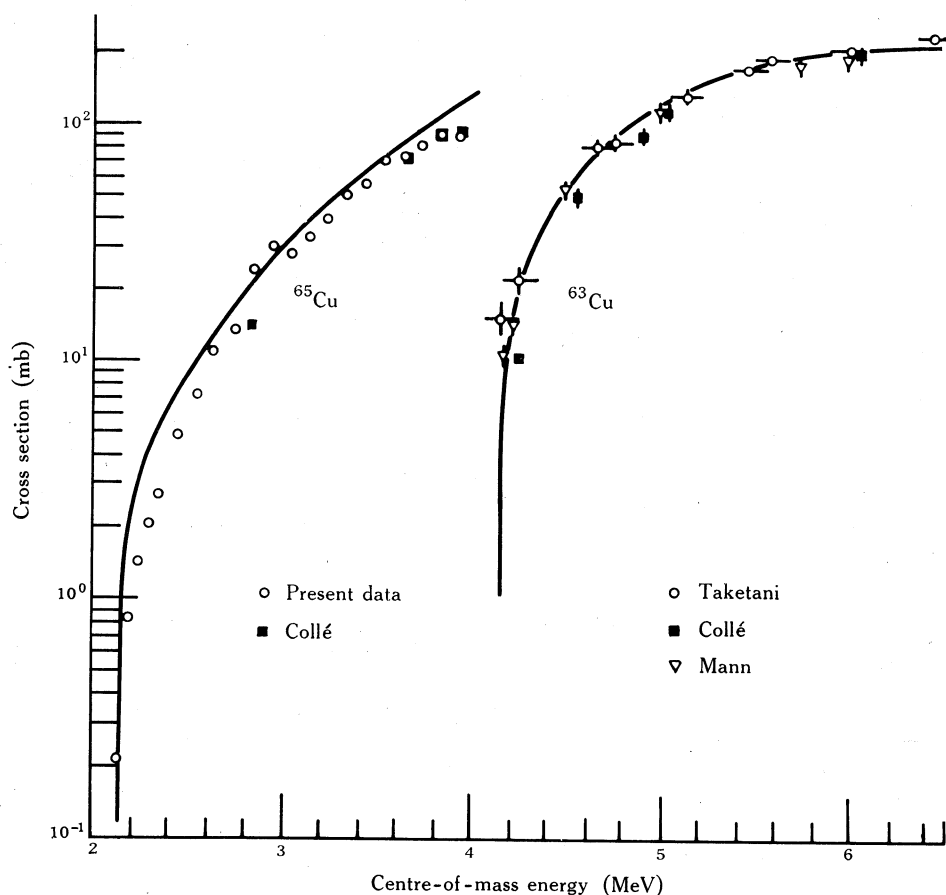


Fig. 3. Excitation functions of proton-induced reactions on (a)  $^{63}\text{Cu}$  and (b)  $^{65}\text{Cu}$ . The  $(p, \gamma)$  data are relative only and have been normalized to the theory. The  $(p, \alpha)$  cross sections are absolute, having been normalized to measured Rutherford scattering. The curves are the results of Hauser-Feshbach statistical model calculations which are described in the text. Error bars represent statistical uncertainties only and, where not explicitly shown, are smaller than the points.



detector to neutrons. Therefore, no information was obtained on the behaviour of  $^{63}\text{Cu}(p, \gamma)^{64}\text{Zn}$  near its neutron threshold.

With reference to the charged-particle work,  $\alpha$ -particle groups from reactions on  $^{63}\text{Cu}$  and  $^{65}\text{Cu}$  were clearly resolved. This follows from the respective  $Q$  values given in Fig. 1. Care was taken to prevent the pile-up of pulses from elastically scattered protons from obscuring the  $(p, \alpha)$  peaks. Measurements were made of the angular distribution of the  $^{65}\text{Cu}(p, \alpha_0)$  reaction at  $E_p = 3$  MeV. The angular distribution was isotropic. Statistical model calculations confirmed that, for the energies pertinent to this experiment, the energy-averaged angular distribution is isotropic to within  $\pm 6\%$ . The absolute total  $(p, \alpha)$  cross sections were then inferred from the measured  $120^\circ$  excitation function by assuming an isotropic distribution.



**Fig. 4.** Excitation functions for  $(p, n)$  reactions on  $^{63}\text{Cu}$  and  $^{65}\text{Cu}$ . The open circles shown for  $^{65}\text{Cu}(p, n)$  represent the results of the present measurements. Other data are taken from Taketani and Alford (1962), Collé *et al.* (1974) and Mann and Kavanagh (1975) as indicated. The curves are the results of statistical model calculations described in the text.

The  $(p, \gamma)$  and  $(p, \alpha)$  yield curves are shown in Fig. 3. Data are plotted against the c.m. energy at the centre of the target. The  $\gamma$ -ray data have been normalized to the results of statistical model calculations which are described in the next section. At low energies the cross sections rise smoothly as the proton energy increases up

the Coulomb barrier. At the crossing of the (p, n) threshold for the  $^{65}\text{Cu}$  case, both (p,  $\gamma$ ) and (p,  $\alpha_0$ ) cross sections fall dramatically. This is the first example where strong cusps have been experimentally observed in both  $\gamma$ -ray and charged-particle channels. In the  $^{63}\text{Cu}$  case, where only the (p,  $\alpha_0$ ) and (p,  $\alpha_1$ ) reactions were studied over the n threshold, there is little change in the general trend of the data.

**Table 1. Optical model parameters**

Data for protons, neutrons and  $\alpha$  particles are from Becchetti and Greenlees (1969), Wilmore and Hodgson (1964) and McFadden and Satchler (1966) respectively

Model parameter	Value of parameter for:		
	protons	neutrons	$\alpha$ particles
$V$ (MeV)	$54 - 0.32E + 24(N-Z)/A + 0.4Z/A^{1/3}$	$47.0 - 0.27E$	185
$W_v$ (MeV)	0	0	25
$W_s$ (MeV)	$11.8 - 0.25E + 12(N-Z)/A$	9.52	0
$r_r$ (fm)	1.17	1.29	1.40
$r_v$ (fm) <sup>A</sup>	1.17	1.29	1.40
$r_s$ (fm)	1.32	1.25	0
$a_r$ (fm)	0.75	0.66	0.52
$a_v$ (fm)	0	0	0.52
$a_s$ (fm)	$0.51 + 0.7(N-Z)/A$	0.48	0

<sup>A</sup> The assignment  $r_v = r_c$  was made throughout.

The (p, n) excitation functions are shown in Fig. 4. The results of the present (normalized) data for  $^{65}\text{Cu}(\text{p}, \text{n})$  agree well with earlier data of Johnson *et al.* (1958) where the energies overlap, i.e. between 2.1 and 2.5 MeV. To permit a more complete comparison with statistical model predictions, an excitation function for the  $^{63}\text{Cu}(\text{p}, \text{n})^{63}\text{Zn}$  reaction has been compiled from the literature, and this is also shown in Fig. 4. Data were obtained from Taketani and Alford (1962) (whose stacked-foil technique introduces an uncertainty in the effective beam energy, which is shown), Collé *et al.* (1974) and Mann and Kavanagh (1975).

**Table 2. Level density parameters**

Level density parameter	Value of parameter for residual nucleus:							
	$^{60}\text{Ni}$	$^{62}\text{Ni}$	$^{63}\text{Cu}$	$^{65}\text{Cu}$	$^{63}\text{Zn}$	$^{64}\text{Zn}$	$^{65}\text{Zn}$	$^{66}\text{Zn}$
$a$	6.4	6.4	6.6	6.2	7.4	7.4	7.0	7.9
$\Delta$ (MeV)	1.3	0.5	-0.5	-0.8	1.1	-1.2	-1.0	-1.2
No. of discrete levels	12	6	9	7	6	9	15	15

#### 4. Statistical Model

The experimental cross sections were compared with Hauser-Feshbach statistical model predictions using the computer code Hauser\*4 (Mann 1976). Since the present measurements represent averages over energy intervals sufficiently broad that statistical fluctuations are damped out, such a comparison should be valid. In the theory of average cross sections, the angle-integrated cross section  $\sigma_{xx}$ , averaged

over compound nucleus fluctuations may be written

$$\sigma_{\alpha\alpha'} = \pi\lambda^2 \sum_{J\pi} \frac{2J+1}{(2I+1)(2i+1)} W_{\alpha\alpha'}^{J\pi} \sum_{sl} T_{\alpha sl}^J \sum_{s'l'} T_{\alpha's'l'}^J / \sum_{\alpha''s''l''} T_{\alpha''s''l''}^J, \quad (3)$$

where the unprimed quantities refer to the entrance channel specified by  $\alpha$ , the singly primed quantities refer to the exit channels specified by  $\alpha'$  and the doubly primed quantities refer to all possible exit channels. Each channel  $\alpha$  has angular momentum  $l$  and channel spins  $s = I+i$  leading to a total angular momentum  $J$ . The transmission functions  $T_{\alpha sl}$  were calculated from the optical model potential appropriate to each pair of particles.

The form of the optical potential employed is

$$U(r) = -Vf(r; R_r, a_r) - iW_v f(r; R_v, a_v) + 4i a_s W_s df(r; R_s, a_s)/dr, \quad (4)$$

where

$$f(r; R_i, a_i) = \{1 + \exp(r - R_i)/a_i\}^{-1} \quad \text{and} \quad R_i = r_i A^{1/3} \quad (5)$$

for  $i = r, v$  and  $s$ . The values assigned to the parameters appearing in equation (4) for the optical potentials for protons, neutrons and  $\alpha$  particles are listed in Table 1. The Coulomb potential used is that of a uniformly charged sphere with radius  $r_c A^{1/3}$ , with  $r_c$  chosen to be identical with  $r_v$ . The photon transmission functions have a different form from that employed for neutrons, protons and  $\alpha$  particles. Details of their calculation have been given by Holmes *et al.* (1976). The function  $W_{\alpha\alpha'}^{J\pi}$  is the width fluctuation correction and may be especially important owing to the relatively few open channels characteristic of the reactions of interest. These factors were calculated according to the approximation of Tepel *et al.* (1974).

In practice, the summation in the denominator of equation (3) is evaluated with the aid of a nuclear level density formula, so that we have

$$\sum_{\alpha''s''l''} T_{\alpha''s''l''}^J = \sum_{E^*=0}^{E_0} T_{\alpha''s''l''}^J + \sum_{I''\pi''} \int_{E_0}^{E^*} \rho(E, I'', \pi'') T_{\alpha''s''l''}^J dE. \quad (6)$$

The transmission coefficients were calculated for the excitation energies of known discrete states of the residual nuclei from  $E^* = 0$  to  $E_0$ . The number of states explicitly included is given in Table 2. For excitation energies above  $E_0$ , the level density was determined from the backshifted Fermi gas formula (Gilbert and Cameron 1965)

$$\rho(E) = \exp(2a^{1/2}(E - \Delta)^{1/2}) / 12\sqrt{2} \sigma a^{1/4} (E - \Delta)^{5/4}. \quad (7)$$

Here,  $E$  is the excitation energy,  $\Delta$  is the pairing energy correction and  $\sigma^2 = \mathcal{I}t/h^2$  is the spin cutoff factor. The nuclear moment of inertia  $\mathcal{I}$  is expressed as the rigid-body moment  $\frac{2}{5}mAR^2$  for  $R = 1.25 A^{1/3}$  fm, where  $m$  is the mass of the nucleon and  $A$  the nuclear mass number. The nuclear temperature  $t$  and the level density parameter  $a$  are related through the equation  $E - \Delta = at^2 - t$ . The spin dependence of the level density is taken to be

$$\rho(E, I) = (2I+1) \rho(E) \frac{1}{2} \sigma^{-2} \exp(-\frac{1}{2} \sigma^{-2} (I + \frac{1}{2})^2) \quad (8)$$

and

$$\rho(E, I, \pi) = \frac{1}{2} \rho(E, I). \quad (9)$$

Values of the level density parameters used for the present calculations are given in Table 2.

The consequences of isospin conservation are not taken into account in the present formulation. The implications of such an omission are discussed more fully elsewhere (Grimes *et al.* 1972; Robson *et al.* 1973). Protons may excite a target nucleus with ground state isospin  $T_0$  to both  $T^< (= T_0 - \frac{1}{2})$  and  $T^> (= T_0 + \frac{1}{2})$  states. To the extent that isospin is a good quantum number, conservation of isospin requires that neutron and  $\alpha$ -particle emission proceed through  $T^<$  states only for bombarding energies near threshold, as in the present experiment. This feature has been recently discussed by Fowler (1976), who points to the use within the statistical model calculations of an isospin mixing parameter  $\mu$  whose value may be adjusted to fit the observed cross sections. The present calculation assumes complete mixing, that is,  $\mu = 1$ .

The results of statistical model calculations using the parameters of Tables 1 and 2 are shown by the curves in Figs 3 and 4. The trends of the two  $(p, \gamma)$  excitation functions are well reproduced by the calculations. The predicted  $^{65}\text{Cu}(p, \gamma)$  cusp faithfully follows the experimental data. There is, in addition, an indication in the data of a further secondary cusp near  $E_{\text{cm}} = 2.95$  MeV, which is attributed by calculation to the opening of the  $(p, n_4)$  channel which populates the  $5/2^-$  state at 770 keV in  $^{65}\text{Zn}$ . The agreement of theory with the  $(p, \alpha)$  data is also good, especially since the absolute magnitudes of the cross sections are predicted correctly. The  $(p, n)$  excitation functions are also well reproduced. No attempt has been made to optimize the fits, as one aim of the present work was to test the use of global parameter sets in statistical model calculations. For the low bombarding energies of interest here, the predictions are insensitive to the details of the level density expressions.

It is interesting to note that the cusps evident in the  $^{65}\text{Cu}(p, \gamma)$  and  $^{65}\text{Cu}(p, \alpha_0)$  reactions arise from the influence of different levels in  $^{65}\text{Zn}$ . This may be understood from simple angular momentum considerations. For low energies, capture of s-wave protons in the entrance channel is most likely. This leads to the population of  $J^\pi = 1^-$  and  $2^-$  states in the  $^{65}\text{Zn}$  compound nucleus. Now s-wave neutron emission to the  $5/2^-$   $^{65}\text{Zn}$  ground state may proceed via the decay of only the  $2^-$  compound states. These unnatural parity levels cannot decay by  $\alpha$ -particle emission. Consequently, a rapid depletion should result in the  $(p, \gamma)$  channel at the crossing of the  $(p, n_0)$  threshold, but essentially no change should occur in the  $(p, \alpha)$  yield. This situation changes at the crossing of the  $1/2^-$  first excited state of  $^{65}\text{Zn}$  at 0.054 MeV. This level may be populated by s-wave neutrons from the  $1^-$  compound states which also decay by  $l = 1$   $\alpha$ -particle emission. The onset of a cusp in the  $(p, \alpha)$  reaction is then delayed by 54 keV from the  $(p, \gamma)$  cusp. This feature is seen clearly in the calculated curves but the present data have insufficient resolution to check this prediction with precision. Similar arguments explain the presence of a secondary cusp in the  $(p, \gamma)$  cross section and the absence of a comparable effect in  $(p, \alpha)$ .

## 5. Conclusions

The Hauser-Feshbach statistical model analysis using global parameter sets is consistent with the  $^{63}\text{Cu} + p$  and  $^{65}\text{Cu} + p$  reaction data reported here. Cross section

measurements of  $^{65}\text{Cu} + p$  reactions in the vicinity of the neutron threshold show evidence of dramatic Wigner cusps. Within the context of stellar nucleosynthesis, these cusps will require special attention. Even when the cusps are smoothed out by thermal averaging, the stellar reaction rates for a reaction dominated by a cusp are difficult to treat analytically. It will be necessary to study more examples before a systematic analytical characterization of reactions showing this behaviour can be formulated.

### Acknowledgments

We are grateful to Professor W. A. Fowler and Professor S. E. Woosley for stimulating comments and correspondence throughout this work. We acknowledge a number of interesting discussions with Dr D. G. Sargood and R. J. Wilkinson. One of us (Z.E.S.) acknowledges receipt of a Queen Elizabeth II Fellowship. This work was supported in part by the Australian Research Grants Committee.

### References

- Bechetti, F. D., and Greenlees, G. W. (1969). *Phys. Rev.* **182**, 1190.  
Collé, R., Kishore, R., and Cumming, J. B. (1974). *Phys. Rev. C* **9**, 1819.  
Fowler, W. A. (1976). Proc. 4th Conf. on Applications of Small Accelerators (Eds J. L. Duggan and I. L. Morgan), p. 11 (IEEE: New York).  
Gilbert, A., and Cameron, A. G. S. (1965). *Can. J. Phys.* **43**, 1446.  
Grimes, S. M., Anderson, J. D., Kerman, A. K., and Wong, C. (1972). *Phys. Rev. C* **5**, 85.  
Hodgson, P. E. (1976). *Nature* **259**, 364.  
Holmes, J. A., Woosley, S. E., Fowler, W. A., and Zimmerman, B. A. (1976). *At. Data Nucl. Data Tables* **18**, 305.  
Jarmie, N., and Allen, R. C. (1959). *Phys. Rev.* **114**, 176.  
Johnson, C. H., Galonsky, A., and Ulrich, J. P. (1958). *Phys. Rev.* **109**, 1243.  
McFadden, L., and Satchler, G. R. (1966). *Nucl. Phys.* **84**, 177.  
Mann, F. M. (1976). Hanford Eng. and Development Lab. Int. Rep. No. HEDL-TME-7680.  
Mann, F. M., Dayras, R. A., and Switkowski, Z. E. (1975). *Phys. Lett. B* **58**, 420.  
Mann, F. M., and Kavanagh, R. W. (1975). *Nucl. Phys. A* **255**, 287.  
Mann, F. M., and Schenter, R. E. (1977). *Nucl. Sci. Eng.* **63**, 242.  
Mann, F. M., and Switkowski, Z. E. (1975). Proc. Conf. on Nuclear Cross Sections and Technology (Eds. R. A. Schrack and C. D. Bowman), p. 354 (NBS: Washington D.C.).  
Paine, B. M., Kennett, S. R., and Sargood, D. G. (1978). *Phys. Rev. C* **17** (in press).  
Presser, G., and Bass, R. (1972). *Nucl. Phys. A* **182**, 321.  
Robson, D., Richter, A., and Harney, H. L. (1973). *Phys. Rev. C* **8**, 153.  
Switkowski, Z. E., Heggie, J. C., and Mann, F. M. (1978). *Phys. Rev. C* **17**, 392.  
Taketani, H., and Alford, W. P. (1962). *Phys. Rev.* **125**, 291.  
Tepel, J. W., Hofmann, H. F., and Weidenmüller, H. A. (1974). *Phys. Lett. B* **49**, 1.  
Votava, H. J., and Thompson, W. J. (1972). *Phys. Lett. B* **41**, 405.  
Wigner, E. P. (1948). *Phys. Rev.* **73**, 1002.  
Wilmore, D., and Hodgson, P. E. (1964). *Nucl. Phys.* **55**, 673.  
Woosley, S. E., Fowler, W. A., Holmes, J. A., and Zimmerman, B. A. (1975). Kellogg Radiation Lab. (Caltech) preprint No. OAP-422.  
Zyskind, J. L., et al. (1977). Proc. Int. Conf. on Nuclear Structure, Tokyo, p. 846 (Int. Academic Printing Co.: Tokyo).

